Synthesis, photophysics, and electrochemistry of hexanuclear silver(I) chalcogenolate complexes. X-Ray crystal structures of $[Ag_6(\mu\text{-dppm})_4(\mu_3\text{-}SC_6H_4Me\text{-}p)_4](PF_6)_2$ and $[Ag_6(\mu\text{-dppm})_4(\mu_3\text{-}SeC_6H_4Cl\text{-}p)_4](PF_6)_2$

Vivian Wing-Wah Yam,* Eddie Chung-Chin Cheng and Nianyong Zhu

Department of Chemistry, The University of Hong Kong, Pokfulam Road, Hong Kong, P. R. China. E-mail: wwyam@hku.hk; Fax: +852 2857 1586; Tel: +852 2859 2153

Received (in Montpellier, France) 20th September 2001, Accepted 6th November 2001
First published as an Advance Article on the web 14th February 2002

A series of unprecedented hexanuclear silver(I) chalcogenolate complexes with bridging dppm ligands, $[Ag_6(\mu\text{-dppm})_4(\mu_3\text{-}EAr)_4](PF_6)_2$ (EAr = SPh **1**, $SC_6H_4Me\text{-}p$ **2**, SePh **3**, $SeC_6H_4Cl\text{-}p$ **4**), have been synthesized and characterized. The X-ray crystal structures of **2** and **4** have been determined. The complexes were found to exhibit luminescence at 77 K and the orange-red emission was tentatively attributed to originate from excited states of an admixture of metal-centred (MC) and metal···metal-bond-to-ligand charge-transfer (MMLCT) character. The complexes were also found to exhibit interesting fluxional behaviour in solution and the weak Ag···Ag interaction is believed to play an important role in governing their fluxional properties.

Transition metal chalcogenolates with a d^{10} electronic configuration have been found to have wide applications and importance in structural chemistry, photocatalysis, medicinal and bioinorganic chemistry.[1] However, reports on the d^{10} transition metal chemistry of this class of compounds are relatively limited owing to the strong tendency of chalcogenolates to bridge metal centres and consequently form insoluble polymers, which precludes purification and characterization. To circumvent the problem of uncontrolled polymerization, an increase in steric demand of the organic chalcogenolate group or incorporation of heteroligands such as phosphines as a "stabilizing agent" on the metal centres have usually been employed. The extreme scarcity of reports on the photophysics of silver(I) chalcogenolate complexes[2] compared to those of other d^{10} metal centres and the unprecedented employment of diphosphine ligands in silver(I) chalcogenolate synthesis have prompted us to extend our recent efforts on the study of transition metal chalcogenolates[3] to that of silver(I). In this article, the synthesis, characterization and luminescence properties of a series of novel, soluble hexanuclear silver(I) thiolate and selenolate complexes with bridging dppm ligands, $[Ag_6(\mu\text{-dppm})_4(\mu_3\text{-}EAr)_4](PF_6)_2$ (EAr = SPh **1**, $SC_6H_4Me\text{-}p$ **2**, SePh **3**, $SeC_6H_4Cl\text{-}p$ **4**), are described. The X-ray crystal structures of a thiolate and a selenolate complex of silver(I) have been determined; the latter represents a rare example of the structural characterization of silver(I) selenolate complexes.[4]

Experimental

Materials and reagents

$NaBH_4$ (98%), NaH (60% in mineral oil), $(SPh)_2$ (99%), $Na(SC_6H_4Me\text{-}p)$ (98%) and $(SeC_6H_4Cl\text{-}p)_2$ (98%) from Aldrich and $(SePh)_2$ (98%) from Strem were used as received. $[Ag_2(\mu\text{-dppm})_2(MeCN)_2](PF_6)_2$ was prepared according to a literature method.[5] THF, CH_2Cl_2 and diethyl ether were purified and distilled according to standard procedures.[6] All other solvents and reagents of analytical grade were used as received.

Syntheses

All reactions and manipulations were performed in an inert atmosphere of nitrogen using standard Schlenk techniques.

$[Ag_6(\mu\text{-dppm})_4(\mu_3\text{-}SPh)_4](PF_6)_2$ (1). Na(SPh) was prepared *in situ* by mixing $(SPh)_2$ (21 mg, 0.096 mmol) and $NaBH_4$ (7.5 mg, 0.20 mmol) in THF (5 ml). The white suspension was stirred for 3 h and was then added to a CH_2Cl_2 solution (20 ml) containing $[Ag_2(\mu\text{-dppm})_2(MeCN)_2](PF_6)_2$ (200 mg, 0.15 mmol). The mixture was stirred for a further 6 h with protection from light and the white precipitate was then filtered off. The colourless filtrate was evaporated to dryness; the white residue was washed with diethyl ether (2×10 ml), redissolved in CH_2Cl_2 (*ca.* 2 ml) and filtered. Slow diffusion of diethyl ether vapour into this concentrated solution afforded white crystals of the product. Subsequent recrystallization by layering methanol over concentrated dichloromethane solution gave **1** as colourless cube-like crystals (121 mg, 85% yield). Positive-ion FAB-MS: $m/z = 2767$ $\{M - PF_6\}^+$. Positive ESI-MS: $m/z = 1310$ $\{M - 2PF_6\}^{2+}$. ^1H NMR (CD_2Cl_2, 300 MHz, 298 K): δ 3.03 (m, 8H, $-CH_2-$), 6.60–7.46 (m, 100H, aromatic H's). $^{31}P\{^1H\}$ NMR (CD_2Cl_2, 202 MHz, 298 K): δ 0.2 (br m, dppm). Anal. calcd for $[Ag_6(dppm)_4(SPh)_4(PF_6)_2]\cdot 1/2CH_2Cl_2$: C 50.62, H 3.72; found: C 50.54, H 3.77.

$[Ag_6(\mu\text{-dppm})_4(\mu_3\text{-}SC_6H_4Me\text{-}p)_4](PF_6)_2$ (2). $[Ag_2(\mu\text{-dppm})_2(MeCN)_2](PF_6)_2$ (200 mg, 0.15 mmol) and $Na(SC_6H_4Me\text{-}p)$ (29 mg, 0.20 mmol) in CH_2Cl_2–MeOH (10 ml : 1 ml) were stirred for 6 h in the dark to give a pale yellow solution. The solvent was removed by evaporation under reduced pressure to dryness and the white solid obtained was dissolved in dichloromethane (5 ml) and filtered; subsequent diffusion of diethyl ether vapour into the concentrated solution yielded **2** as white crystals (134 mg, 91% yield). Positive-ion FAB-MS: $m/z =$ 2437 $\{M - dppm - PF_6\}^+$. Positive ESI-MS: $m/z = 1338$ $\{M - 2PF_6\}^{2+}$. ^1H NMR (CD_2Cl_2, 300 MHz, 298 K): δ 2.32 (s, 12H, $-CH_3$), 3.05 (m, 8H, $-CH_2-$), 6.79–7.31 (m, 96H, aromatic H's). $^{31}P\{^1H\}$ NMR (CD_2Cl_2, 202 MHz, 298 K): δ −0.1 (br m, dppm). Anal. calcd for $[Ag_6(dppm)_4(SC_6H_4Me)_4](PF_6)_2\cdot MeOH$: C 51.65, H 4.03; found: C 51.56, H 4.17.

This journal is © The Royal Society of Chemistry and the Centre National de la Recherche Scientifique 2002

$[Ag_6(\mu\text{-dppm})_4(\mu_3\text{-}SeC_6H_5)_4](PF_6)_2$ (3). This was prepared by a method similar to that of **1** except $(SePh)_2$ (31 mg, 0.099 mmol) was used instead of $(SPh)_2$. **3** was recrystallized by slow diffusion of diethyl ether vapour into a concentrated CH_2Cl_2 solution of **3** as yellow needle-like crystals (144 mg, 95% yield). Positive FAB-MS: $m/z = 2958$ $\{M - PF_6\}^+$. Positive ESI-MS: $m/z = 1404$ $\{M - 2PF_6\}^{2+}$. ^1H NMR (CD_2Cl_2, 300 MHz, 298 K): δ 3.09 (m, 8H, $-CH_2-$); 6.60–7.54 (m, 100H, aromatic H's). $^{31}P\{^1H\}$ NMR (CD_2Cl_2, 202 MHz, 298 K): $\delta - 1.3$ (br m, dppm). Anal. calcd for $Ag_6(dppm)_4(SePh)_4(PF_6)_2 \cdot CH_2Cl_2$: C 47.15, H 3.48; found: C 47.05, H 3.41.

$[Ag_6(\mu\text{-dppm})_4(\mu_3\text{-}SeC_6H_4Cl\text{-}p)_4](PF_6)_2$ (4). The procedure was similar to that of **1** except $(SeC_6H_4Cl\text{-}p)_2$ (38 mg, 0.10 mmol) was used to give yellow crystals of **4** (95 mg, 60% yield). Positive-ion FAB-MS: $m/z = 3093$ $\{M - PF_6\}^+$. Positive ESI-MS: $m/z = 1473$ $\{M - 2PF_6\}^{2+}$. ^1H NMR (CD_2Cl_2, 300 MHz, 298 K): δ 3.17 (m, 8H, $-CH_2-$), 6.79–7.35 (m, 96H, aromatic H's). $^{31}P\{^1H\}$ NMR (CD_2Cl_2, 202 MHz, 298 K): $\delta - 0.3$ (br m, dppm). Anal. calcd for $Ag_6(dppm)_4(SeC_6H_4Cl)_4(PF_6)_2$: C 46.01, H 3.24; found: C 45.90, H 3.13.

Physical measurements and instrumentation

^1H NMR spectra were recorded on a Bruker DPX-300 (300 MHz) FT-NMR spectrometer with chemical shifts quoted relative to tetramethylsilane, $SiMe_4$. ^{31}P NMR spectra were recorded on a Bruker DRX-500 (202 MHz) FT-NMR spectrometer with chemical shifts quoted relative to 85% H_3PO_4 (external standard). Positive-ion fast-atom bombardment (FAB) mass spectra were recorded on a Finnigan MAT95 mass spectrometer, and positive electrospray ionization (ESI) mass spectra on a Finnigan LCQ mass spectrometer. Elemental analyses were performed on a Carlo Erba 1106 elemental analyzer at the Institute of Chemistry in Beijing, Chinese Academy of Sciences.

The electronic absorption spectra were obtained on a Hewlett–Packard 8452A diode array spectrophotometer. Steady state emission spectra recorded at 77 K were obtained on a Spex Fluorolog-2 Model F111 fluorescence spectrophotometer with or without Corning filters. Low temperature (77 K) solid-state and glass photophysical measurements were carried out with the solid sample loaded in a quartz tube inside a quartz-walled Dewar flask filled with liquid nitrogen. Luminescence lifetime measurements were performed using a conventional laser system. The excitation source was the 355 nm output (third harmonic) of a Spectra-Physics Quanta-Ray Q-switched GCR-150-10 pulsed Nd-YAG laser. Luminescence decay signals were detected by a Hamamatsu R928 photomultiplier tube and recorded on a Tektronix Model TDS-620A (500 MHz, 2 GS/s) digital oscilloscope, and analyzed using a program for exponential fits on an IBM-compatible PC-computer.

Cyclic voltammetric measurements were performed by using a CH Instruments, Inc. model CHI 620 electrochemical analyzer interfaced to an IBM-compatible personal computer. The electrolytic cell used was a conventional two-compartment cell. The salt bridge of the reference electrode was separated from the working electrode compartment by a Vycor glass. Electrochemical measurements were performed in MeCN solutions (0.1 M $^nBu_4NPF_6$) with $Ag/AgNO_3$ (0.1 M in MeCN) as the reference electrode. The ferrocenium-ferrocene couple was used as the internal standard in the electrochemical measurements in MeCN.[7] The working electrode was a glassy carbon (Atomergic Chemetals V25) electrode with a platinum wire acting as the counter electrode. The working electrode surface was first polished with 1 μm α-alumina slurry (Linde) on a microcloth (Buehler Co.). It was then rinsed with nano-pure deionized water and sonicated in a beaker containing nano-pure water for 5 min. The polishing and sonicating procedures were repeated using the 0.3 μm α-alumina slurry (Linde). All the solutions for electrochemical studies were deaerated using pre-purified argon gas.

Crystal structure determination

Single crystals of **2** and **4** suitable for diffraction studies were grown by slow diffusion of diethyl ether vapour into concentrated CH_2Cl_2 solutions of the respective complexes. Crystals were mounted in a glass capillary saturated with the mother liquor and used for data collection at 28 °C on a MAR diffractometer with a 300 mm image plate detector using graphite monochromated Mo-Kα radiation ($\lambda = 0.71073$ Å). Data collection was made with 2° oscillation step of φ, 300 s exposure time and scanner distance at 120 mm. For **2** and **4** 110 and 36 images, respectively, were collected.

The images were interpreted and intensities integrated using the program DENZO.[8] The structures were solved by direct methods employing the program SHELXS-97 on PC.[9] The Ag, Se, P and some C atoms were located by direct methods. The positions of the other non-hydrogen atoms were found after successful refinement by full-matrix least-squares using the SHELXL-97 program for PC.[9] In each compound, the P atoms of the two PF_6^- anions were located in special positions. Only two unique positions for each set of six F atoms were found. F(1) and F(2) were bound to P(3), in which F(2) was on a special position (0.5 occupancy) and F(1) in a normal position. F(3) and F(4) were bound to P(4), but neither of them was on a special position; therefore the occupancy of each of them was set to 0.75.

One crystallographic asymmetric unit consisted of one fourth of one formula unit for each compound. In the final stage of least-squares refinement, all non-hydrogen atoms were refined anisotropically. H atoms were generated by the program SHELXL-97.[9] The positions of H atoms were calculated based on riding mode with thermal parameters equal to 1.2 times that of the associated C atoms, and were included in the calculation of the final R indices. Since the structure refinements were performed against F^2, the R indices based on F^2 were larger than (more than double) those based on F. For comparison with older refinements based on F and the OMIT threshold, a conventional index R_1 based on observed F values larger than $4\sigma(F_o)$ is also given [corresponding to Intensity $\geqslant 2\sigma(I)$]. $wR_2 = \{\Sigma[w(F_o^2 - F_c^2)^2]/\Sigma[w(F_o^2)^2]\}^{1/2}$, $R_1 = \Sigma||F_o| - |F_c||/\Sigma|F_o|$. The weighting scheme was: $w = 1/[\sigma^2(F_o^2) + (aP)^2 + bP]$, where $P = [2F_c^2 + \mathrm{Max}(F_o^2, 0)]/3$.

CCDC reference numbers 171524 (for **2**) and 171525 (for **4**). See http://www.rsc.org/suppdata/nj/b1/b108759m/ for crystallographic data in CIF or other electronic format.

Results and discussion

Syntheses and characterization

Treatment of two equivalents of a solution of the sodium salts of chalcogenolate with three equivalents of $[Ag_2(\mu\text{-dppm})_2(MeCN)_2](PF_6)_2$ in CH_2Cl_2 under anhydrous and anaerobic conditions resulted in the formation of a series of unprecedented hexanuclear silver(I) thiolate and selenolate complexes with bridging dppm ligands, having the general formula $[Ag_6(\mu\text{-dppm})_4(\mu_3\text{-}EAr)_4](PF_6)_2$ (EAr = SPh **1**, $SC_6H_4Me\text{-}p$ **2**, SePh **3** and $SeC_6H_4Cl\text{-}p$ **4**). The reaction mixture was filtered and the solvents were removed under reduced pressure. Subsequent washings of the residue with diethyl ether and recrystallization from the diffusion of diethyl ether vapour into the concentrated CH_2Cl_2 solutions of the complexes afforded analytically pure crystals of the desired products. All the newly synthesized complexes gave satisfactory elemental analyses

and were characterized by positive-ion FAB-MS, positive ESI-MS, ^{1}H and ^{31}P NMR spectroscopy.

The $^{31}P\{^1H\}$ NMR spectra of complexes **1**–**4** at room temperature showed a very broad, unresolved multiplet in the range of $\delta -1.3$ to 0.2. A preliminary correlation of the chemical shift values of the ^{31}P signals with the nature of the chalcogenolate ligands shows a trend of $\mathbf{3} < \mathbf{4} < \mathbf{2} < \mathbf{1}$, which appears to be in line with the electron-donating ability of the chalcogenolate ligands even though the differences are small. The relatively more upfield shift of **3** than **4** is ascribed to the greater electron-donating ability of SePh than SeC_6H_4Cl-*p*. The same argument could also be applied to the observed trend in the chemical shifts between **1** and **2**. Similarly, the more upfield ^{31}P resonances in the selenolate complexes **3** and **4** relative to the thiolate complexes **1** and **2** are in accord with the greater electron-donating ability of the selenolates over the thiolates. The broadening of the resonance signals may suggest the presence of some fluxional processes, which were further complicated by the couplings among the phosphorus atoms themselves as well as with the Ag-107/109 nuclei.

In order to have a clearer understanding of the process taking place and of the structure of the complexes, variable temperature $^{31}P\{^1H\}$ NMR experiments on complexes **1**–**4** were performed. The $^{31}P\{^1H\}$ NMR spectrum of **1** in CD_2Cl_2 at 308 K, which is the highest possible temperature that could be attained in CD_2Cl_2, showed a broad multiplet at *ca.* δ 0.66 (Fig. 1). The signal was split into two broad signals at δ 0.26 and 2.60 upon lowering the temperature to 290 K. As the temperature was further lowered, the signals appeared as a pseudo-triplet at 273 K, an unresolved doublet of doublets at 223 K and an unresolved doublet of doublets at 203 K, a temperature that is close to the freezing point of dichloromethane. Due to the complex nature of the resonance signal pattern, an accurate determination of the coalescence temperature was difficult.

Based on the structural and chemical similarity of complexes **1**–**4**, it is reasonable to believe that they would exhibit similar fluxional behaviour and coupling patterns. So after a careful consideration of the different working temperature ranges of the NMR solvents as well as the solubility and stability of the complexes in various solvents, CD_3CN was chosen as the NMR solvent for the experiments on complexes **2**–**4**. The $^{31}P\{^1H\}$ NMR spectrum of **2** in CD_3CN at 330 K showed a septet pattern centred at δ 1.56 with signal intensities in the expected ratio 1 : 6 : 15 : 20 : 15 : 6 : 1. When the temperature was lowered to 310 K, the signal became an unresolved and broad resonance at δ 1.51. As the temperature was lowered further and approaching 285 K, in addition to the main resonance signals at *ca.* δ 1.4, prominent bands at *ca.* δ 0.6 and 3.5 appeared. A poorly resolved pseudo-triplet at δ 1.79 resulted when the temperature reached 240 K, which is close to the freezing point of acetonitrile. The $^{31}P\{^1H\}$ NMR spectra of **3** (Fig. 2) and **4** in CD_3CN also showed similar changes in the resonance patterns upon lowering of temperature. For **3**, a septet coupling pattern could be observed at δ 0.17 at 338 K, which began to broaden and gave a broad signal at δ 0.17 at 305 K. The signal continued to show a complicated pattern upon lowering of temperature and finally gave a poorly resolved pseudo-triplet centred at $\delta -0.16$ at 240 K. Similarly, for **4**, the septet at δ 1.43 at 318 K became an unresolved multiplet at δ 1.02 as the temperature was lowered to 302 K, which then appeared as a poorly resolved pseudo-triplet centred at δ 0.47 at 238 K. Additional experiments showed that the changes in resonance patterns are thermally reversible, or to be more exact, no signs of thermal decomposition of the complexes have been observed, whether the experiments were performed starting from the high or the low working temperature end.

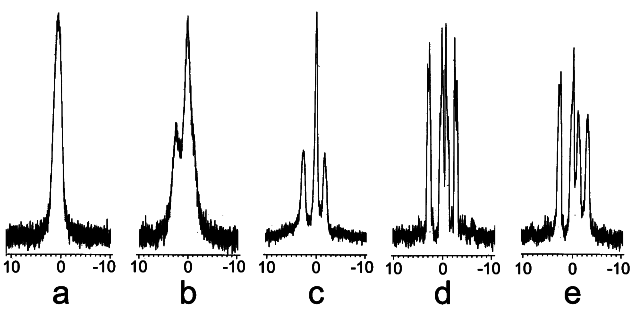

Fig. 1 $^{31}P\{^1H\}$ NMR spectra of $[Ag_6(\mu\text{-dppm})_4(\mu_3\text{-SPh})_4](PF_6)_2$ (**1**) in CD_2Cl_2 at (a) 308 K, (b) 290 K, (c) 273 K, (d) 223 K and (e) 203 K.

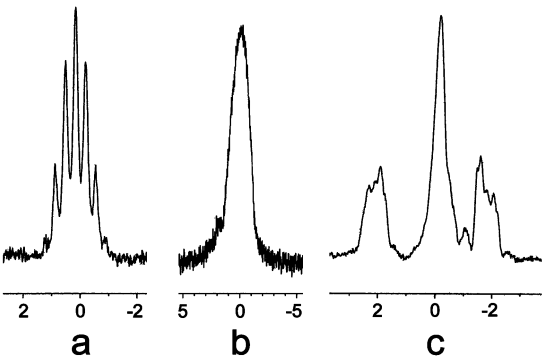

Fig. 2 $^{31}P\{^1H\}$ NMR spectra of $[Ag_6(\mu\text{-dppm})_4(\mu_3\text{-SePh})_4](PF_6)_2$ (**3**) in CD_3CN at (a) 338 K, (b) 305 K and (c) 240 K.

Such a series of changes in the resonance signals observed in the $^{31}P\{^1H\}$ NMR spectra of complexes **1**–**4** upon lowering the temperature can be visualized as the following. At a temperature higher than the room temperature, the complexes undergo extremely rapid phosphine scrambling at a rate that cannot be resolved and monitored within the NMR time-scale. Because of this, the difference between Ag-107 and Ag-109 cannot be distinguished and hence the eight equivalent phosphorus atoms couple to the six equivalent silver atoms to give a septet in the ^{31}P NMR spectrum. At low temperature, the phosphine scrambling process is relatively slow, and so the silver atoms are no longer equivalent. Also, at this stage, two phosphorus environments are present. As a result, two phosphorus resonances are observed, each of which is split by the Ag-107/109 nuclei to give a doublet of doublets. A proposed phosphine scrambling mechanism for the hexanuclear silver(I) chalcogenolate complexes **1**–**4** is given in Fig. 3, which illustrates the exchange of the phosphorus environments P_A and P_B during the process.

Crystal structure determination

Table 1 summarizes the crystal structure determination data of **2** and **4**. The perspective drawings of the complex cations of **2** and **4** with atomic numbering scheme are depicted in Fig. 4 and 5, respectively. The Ag_4E_4 [E = S (**2**), Se (**4**)] unit forms a distorted cubane core and the remaining two silver atoms are capped onto the opposite faces of the cubane, each of them being linked to two bridging dppm ligands. The four chalcogen atoms show an asymmetric μ_3-bonding mode with different Ag–E bond distances and Ag–E–Ag bond angles. The Ag–E bond distances in the distorted cubane core have a value of 2.4904(13) Å in **2** and 2.5922(11) Å in **4**. Thus, each capping silver atom assumes a distorted tetrahedral geometry, with relatively long Ag–E bond distances and short Ag–P bond distances [**2**: Ag–S 2.7021(13) Å, Ag–P 2.4959(13) Å; **4**: Ag–Se 2.7960(11) Å, Ag–P 2.4851(18) Å] (Table 2), when compared to the commonly observed values.[10] The Ag–S bond distances

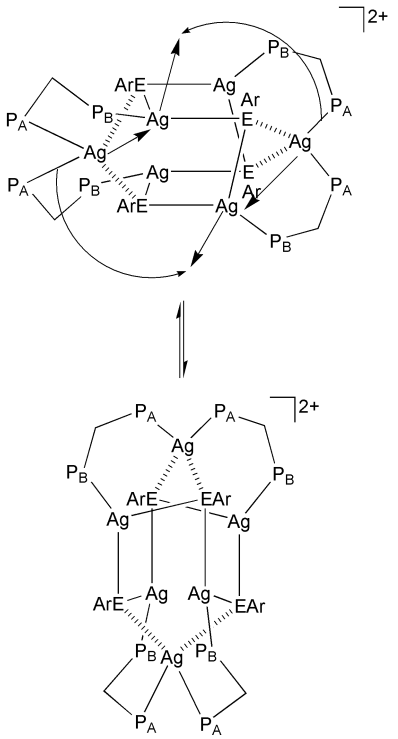

Fig. 3 Proposed mechanism for the dppm scrambling process of complexes **1**–**4** in solution.

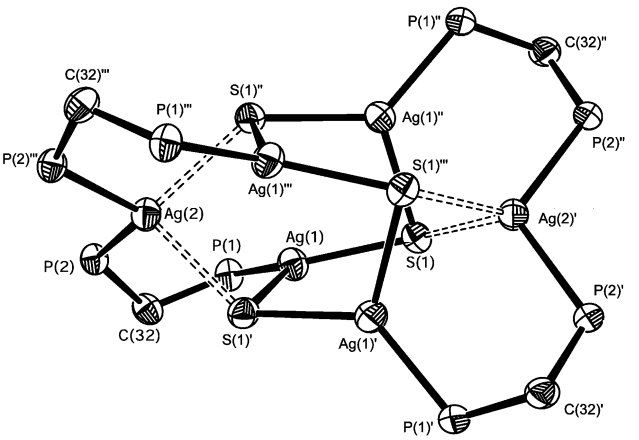

Fig. 4 Perspective drawing of the complex cation in $[Ag_6(\mu\text{-dppm})_4(\mu_3\text{-}SC_6H_4Me\text{-}p)_4](PF_6)_2$ (**2**) with the atomic numbering scheme. Hydrogen atoms and the aromatic rings have been omitted for clarity. Thermal ellipsoids are shown at the 30% probability level.

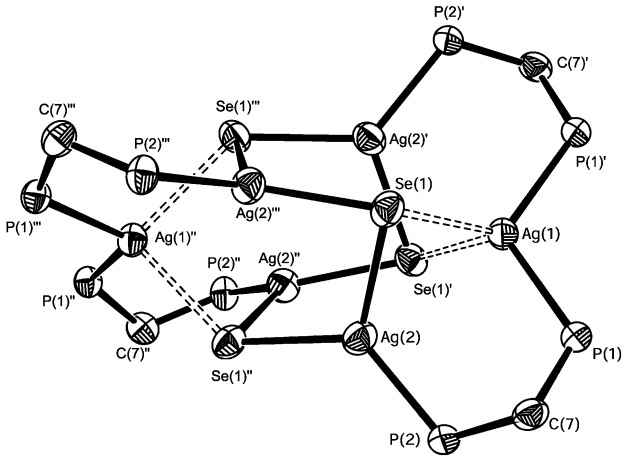

Fig. 5 Perspective drawing of the complex cation in $[Ag_6(\mu\text{-dppm})_4(\mu_3\text{-}SeC_6H_4Cl\text{-}p)_4](PF_6)_2$ (**4**) with the atomic numbering scheme. Hydrogen atoms and the aromatic rings have been omitted for clarity. Thermal ellipsoids are shown at the 30% probability level.

in **2** are generally shorter than the Ag–Se distances in **4**, in accord with the larger size of the selenium atoms over the sulfur atoms. A dihedral angle of 90° is observed between the two Ag_3 planes {Δ[Ag(1)–Ag(1)‴–Ag(2)] *vs.* Δ[Ag(1)′–Ag(1)″–Ag(2)′] in **2** and Δ[Ag(1)″–Ag(2)″–Ag(2)‴] *vs.* Δ[Ag(1)–Ag(2)–Ag(2)′] in **4**}. Short Ag···Ag contacts of 3.3289–3.4768 Å in **2** and 3.3549–3.5184 Å in **4** are observed, which may be indicative of the presence of weak metal···metal interactions when compared to the sum of van der Waals radii for silver (3.4 Å). Similar findings were not observed in the isostructural hexanuclear copper(I) selenolate complexes reported by one of us, where the copper–copper distances in $[Cu_6(\mu\text{-dppm})_4(\mu_3\text{-}SePh)_4](PF_6)_2$ are in the range 3.284(1)–3.325(5) Å, which are substantially longer than the sum of van der Waals radii for copper (2.8 Å) and are suggestive of no copper–copper interactions.[3a] Such a difference in the extent of metal···metal interactions might also account for the difference in fluxional behaviour for the silver complexes *versus* the copper complexes as observed in the solution state $^{31}P\{^1H\}$ NMR studies, in which the presence of weak Ag···Ag interactions would stabilize the transition state for the fluxional process, as mentioned earlier.

Table 1 Crystal and structure determination data for $[Ag_6(\mu\text{-dppm})_4(\mu_3\text{-}SC_6H_4Me\text{-}p)_4](PF_6)_2$ (**2**) and $[Ag_6(\mu\text{-dppm})_4(\mu_3\text{-}SeC_6H_4Cl\text{-}p)_4](PF_6)_2$ (**4**)

	2	**4**
Empirical formula	$[(C_{128}H_{116}Ag_6P_8S_4)^{2+}\cdot 2PF_6^-]$	$[(C_{124}H_{104}Ag_6Cl_4P_8Se_4)^{2+}\cdot 2PF_6^-]$
Formula weight	2967.37	3236.63
Crystal system	Tetragonal	Tetragonal
Space group	$I\bar{4}$ (No. 82)	$I\bar{4}$ (No. 82)
a/Å	16.140(2)	16.021(2)
c/Å	27.624(4)	27.512(4)
U/Å^3	7195.5(16)	7061.6(16)
Z	2	2
μ/mm^{-1}	1.027	2.094
Reflections collected	29 063	8251
Independent reflections	6660	5010
R_{int}	0.0445	0.0352
R_1 $[I > 2\sigma(I)]$	0.0390	0.0374
wR_2 $[I > 2\sigma(I)]$	0.1093	0.0984

Table 2 Selected bond distances (Å) and bond angles (°) with estimated standard deviations (esd's) in parentheses for $[Ag_6(\mu\text{-dppm})_4(\mu_3\text{-}SC_6H_4Me\text{-}p)_4](PF_6)_2$ (**2**) and $[Ag_6(\mu\text{-dppm})_4(\mu_3\text{-}SeC_6H_4Cl\text{-}p)_4](PF_6)_2$ (**4**)

2[a]		**4**[b]	
Ag(1)···Ag(2)	3.3288(6)	Ag(1)···Ag(2)	3.3548(10)
Ag(2)···Ag(1)‴	3.3288(6)	Ag(1)···Ag(2)′	3.3548(10)
Ag(1)···Ag(1)′	4.218(1)	Ag(2)···Ag(2)′	4.209(3)
Ag(1)···Ag(1)″	3.477(1)	Ag(2)···Ag(2)″	3.518(3)
Ag(1)–P(1)	2.4151(13)	Ag(1)–P(1)′	2.4852(18)
Ag(2)–P(2)	2.4959(11)	Ag(1)–P(1)	2.4852(18)
Ag(2)–P(2)‴	2.4959(11)	Ag(2)–P(2)	2.432(2)
Ag(1)–S(1)	2.4906(13)	Ag(1)–Se(1)	2.7960(10)
Ag(1)–S(1)′	2.5557(13)	Ag(1)–Se(1)′	2.7960(10)
Ag(1)″–S(1)	2.5557(13)	Ag(2)–Se(1)″	2.5921(11)
Ag(2)′–S(1)	2.7021(13)	Ag(2)–Se(1)	2.6453(11)
Ag(2)–S(1)′	2.7021(13)	Ag(2)‴–Se(1)	2.5921(11)
Ag(2)–S(1)″	2.7021(13)		
P(1)–Ag(1)–S(1)	130.86(5)	P(1)′–Ag(1)–P(1)	113.51(9)
P(1)–Ag(1)–S(1)′	119.62(4)	P(1)′–Ag(1)–Se(1)	118.86(5)
S(1)–Ag(1)–S(1)′	107.95(4)	P(1)–Ag(1)–Se(1)	106.20(5)
P(1)–Ag(1)–Ag(2)	88.21(3)	P(1)′–Ag(1)–Se(1)′	106.20(5)
S(1)–Ag(1)–Ag(2)	133.38(3)	P(1)–Ag(1)–Se(1)′	118.86(5)
S(1)′–Ag(1)–Ag(2)	52.70(3)	Se(1)–Ag(1)–Se(1)′	92.00(4)
Ag(1)–S(1)–Ag(1)″	87.09(4)	P(1)′–Ag(1)–Ag(2)	161.92(5)
C(1)–S(1)–Ag(2)′	114.48(18)	P(1)–Ag(1)–Ag(2)	84.45(4)
Ag(1)–S(1)–Ag(2)′	137.78(5)	Se(1)–Ag(1)–Ag(2)	49.94(2)
Ag(1)″–S(1)–Ag(2)′	78.51(3)	Se(1)′–Ag(1)–Ag(2)	64.00(3)
P(2)‴–Ag(2)–P(2)	112.52(5)	P(1)′–Ag(1)–Ag(2)′	84.45(4)
P(2)‴–Ag(2)–S(1)′	120.99(4)	P(1)–Ag(1)–Ag(2)′	161.92(5)
P(2)–Ag(2)–S(1)′	106.13(4)	Se(1)–Ag(1)–Ag(2)′	64.00(3)
P(2)‴–Ag(2)–S(1)″	106.13(4)	Se(1)′–Ag(1)–Ag(2)′	49.94(2)
P(2)–Ag(2)–S(1)″	120.99(4)	Ag(2)–Ag(1)–Ag(2)′	77.70(3)
S(1)′–Ag(2)–S(1)″	88.95(6)	P(2)–Ag(2)–Se(1)″	128.02(6)
P(2)‴–Ag(2)–Ag(1)	162.98(3)	P(2)–Ag(2)–Se(1)	119.58(6)
P(2)–Ag(2)–Ag(1)	84.44(3)	Se(1)″–Ag(2)–Se(1)	110.16(3)
S(1)′–Ag(2)–Ag(1)	48.79(3)	P(2)–Ag(2)–Ag(1)	87.50(5)
S(1)″–Ag(2)–Ag(1)	63.56(3)	Se(1)″–Ag(2)–Ag(1)	136.89(3)
P(2)‴–Ag(2)–Ag(1)‴	84.44(3)	Se(1)–Ag(2)–Ag(1)	53.99(2)
P(2)–Ag(2)–Ag(1)‴	162.98(3)	Ag(2)‴–Se(1)–Ag(2)	84.40(3)
S(1)′–Ag(2)–Ag(1)‴	63.56(3)	Ag(2)‴–Se(1)–Ag(1)	133.89(4)
S(1)″–Ag(2)–Ag(1)‴	48.79(3)	Ag(2)–Se(1)–Ag(1)	76.07(3)
Ag(1)–Ag(2)–Ag(1)‴	78.637(19)		

[a] Symmetry transformations used to generate equivalent atoms: ′: $y-\frac{1}{2}$, $-x+\frac{1}{2}$, $-z+\frac{1}{2}$; ″: $-y+\frac{1}{2}$, $x+\frac{1}{2}$, $-z+\frac{1}{2}$; ‴: $-x$, $-y+1$, z. [b] Symmetry transformations used to generate equivalent atoms: ′: $-x+1$, $-y+1$, z; ″: y, $-x+1$, $-z+2$; ‴: $-y+1$, x, $-z+2$.

Electronic absorption and photophysical properties

The electronic absorption properties of the hexanuclear silver(I) chalcogenolate complexes have been studied and the electronic absorption spectral data are tabulated in Table 3. The electronic absorption spectra in CH_2Cl_2 are rather featureless and are characterized by an absorption shoulder at *ca.* 260–262 nm, which is assigned as an intraligand (IL) transition of the dppm ligand. Excitation of solid samples and solutions of complexes **1**–**4** at room temperature did not produce any remarkable luminescence. However, at 77 K, complexes **1**–**4** gave intense luminescence upon excitation at $\lambda \approx 330$ nm (Table 3). The solid state emission spectra of complexes **1**–**4** show an orange-red emission at *ca.* 666–746 nm (Fig. 6). Excitation bands at *ca.* 345–415 nm were observed upon monitoring at the emission maxima. Such a large Stokes shift in energy may suggest that the excited states are highly distorted from those of the ground state. The solid state emission energies of the complexes follow the order: **1** < **2** < **4** < **3**, which is in line with the electron-richness of the chalcogenolate group: SPh < SC_6H_4Me-*p*, SeC_6H_4Cl-*p* < SePh and SPh < SePh. The observation of such a trend is suggestive of the dependence of emission energies on the π-accepting ability of the arenechalcogenolate ligands, in which the thioarene is a slightly better π-acceptor than the selenoarene. Similarly, the chloro-substituted arene is a better π-acceptor than the unsubstituted arene, which then is a better π-acceptor than the methyl-substituted arene. Two assignments are possible. One involves an emission origin that is derived from a MC (ds/dp) transition, since the attachment of a better electron-donating chalcogenolate would render the silver(I) more

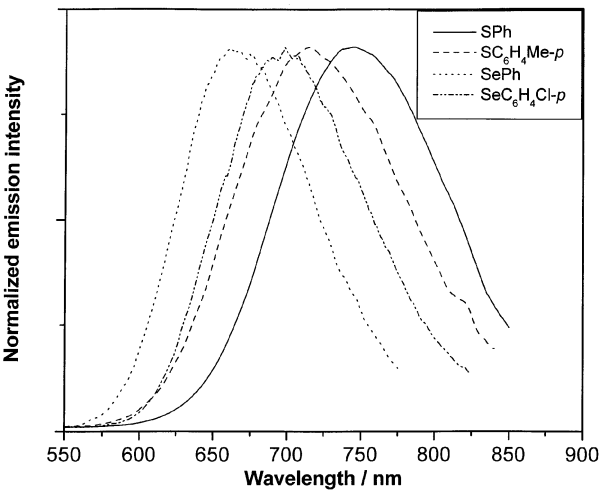

Fig. 6 Solid state emission spectra of $[Ag_6(\mu\text{-dppm})_4(\mu_3\text{-EAr})_4](PF_6)_2$ [EAr = SPh (**1**) (——), SC_6H_4Me-*p* (**2**) (- - - -), SePh (**3**) (·····), SeC_6H_4Cl-*p* (**4**) (-·-·-·)] at 77 K.

Table 3 Electronic absorption, photophysical and electrochemical data for complexes **1**–**4**

		Emission at 77 K		
Complex	λ_{abs}[a]/nm (ε/dm^3 mol^{-1} cm^{-1})	Medium	λ_{em}[b]/nm (τ_o[c]/μs)	Oxidation[d] E_{pa}[e]/V *vs.* SCE
$[Ag_6(\mu\text{-dppm})_4(\mu_3\text{-SPh})_4](PF_6)_2$ (**1**)	260 sh (98 390)	Solid	746 (11.0, 2.5)	+1.11, +1.59
		CH_2Cl_2[f]	566 (225)	
$[Ag_6(\mu\text{-dppm})_4(\mu_3\text{-}SC_6H_4Me\text{-}p)_4](PF_6)_2$ (**2**)	260 sh (102 330)	Solid	716 (320)	+1.05, +1.54
		CH_2Cl_2[f]	578 (290, 65)	
$[Ag_6(\mu\text{-dppm})_4(\mu_3\text{-SePh})_4](PF_6)_2$ (**3**)	260 sh (104 230)	Solid	666 (11.9, 2.6)	+1.05, +1.35
		CH_2Cl_2[f]	568 (11.0, 2.0)	
$[Ag_6(\mu\text{-dppm})_4(\mu_3\text{-}SeC_6H_4Cl\text{-}p)_4](PF_6)_2$ (**4**)	262 sh (105 010)	Solid	695 (13.5, 2.2)	+0.98, +1.41
		CH_2Cl_2[f]	569 (12.5, 1.9)	

[a] In CH_2Cl_2 at 298 K. [b] Corrected for PMT response. [c] Recorded with an uncertainty of ± 10%. [d] In MeCN (0.1 mol dm^{-3} ^{n}Bu$_4$NPF$_6$) at 298 K; glassy carbon working electrode; scan rate 100 mV s^{-1}. [e] E_{pa} is the anodic peak potential of the irreversible oxidation wave. [f] One referee raised a concern about the possibility of the complexes being dispersed as small solid particles in CH_2Cl_2 at 77 K as CH_2Cl_2 would not form a good optical glass at low temperature. We do not favour this possibility since the concentrations of the solutions used were very dilute (~10^{-5} M) and the data were very different from those observed for the solid state samples.

electron-rich, causing a larger charge–charge repulsion on the silver and hence a smaller $Ag^{I}\cdots Ag^{I}$ bonding interaction. This would cause a smaller dσ–dσ*, sσ–sσ* and pσ–pσ* orbital splitting, and hence a larger dσ*–sσ and dσ*–pσ energy gap, leading to an increase in the transition energy. Another possible assignment for the emission origin is derived from excited states of a metal-to-ligand charge transfer (MLCT) [Ag → EAr/phosphine] or MMLCT [Ag···Ag → EAr/phosphine] character, such that chalcogenoarenes with better π-accepting ability would give rise to lower emission energies, similar to the emission trend observed. Since neither of the emission origins could be eliminated and are equally likely, it is therefore not unreasonable to assign the emission origin as derived from excited states with an admixture of MMLCT and MC (ds/dp) character, as (1) the changes in emission energies are prominent upon a change in the chalcogenolate groups, and (2) fairly short Ag···Ag contacts of *ca.* 3.3 Å are observed in the crystal structures of **2** and **4**.

Electrochemical properties

The electrochemical properties of complexes **1**–**4** have been investigated by cyclic voltammetry and the electrochemical data are summarized in Table 3. No observable reduction waves were found upon reductive scan to *ca.* −2.0 V *vs.* SCE. All the complexes show two irreversible oxidation waves at *ca.* +1.0 V and +1.4 to +1.6 V *vs.* SCE. The first oxidation appeared to be rather insensitive towards a systematic change of the chalcogenolate ligands of differing electron-donating abilities in complexes **1**–**4**, and as a result a tentative assignment of a metal-centred $Ag^{+} \rightarrow Ag^{2+}$ oxidation has been made. Such an assignment is consistent with the assignment suggested in the photophysical studies, in which the HOMO has predominantly silver(I) character. The second irreversible oxidation wave, which occurred at more positive potentials, is attributed to the chalcogenolate-centred oxidation. Such an assignment is based on the observation of a more obvious dependence of potential values upon a change of the chalcogenolate ligands. The oxidation potential is in the order: **3** (+1.35 V) < **4** (+1.41 V) < **2** (+1.54 V) < **1** (+1.59 V), in line with the decreasing electron-richness of the chalcogenolate ligands, where SePh > SeC_6H_4Cl-*p*; SePh > SPh and SC_6H_4Me > SPh, as reflected by the $^{31}P\{^{1}H\}$ NMR studies, and hence the reducing ease of oxidation.

Acknowledgements

V. W.-W. Y acknowledges financial support from the Research Grants Council and The University of Hong Kong. E. C.-C. C. acknowledges the receipt of a University Postdoctoral Fellowship from The University of Hong Kong.

References

1 *Sulfur: Its Significance for Chemistry, for the Geo-, Bio- and Cosmosphere and Technology*, ed. A. Muller and B. Krebs, Elsevier, Amsterdam, 1984.
2 F. Sabin, C. K. Ryu, P. C. Ford and A. Vogler, *Inorg. Chem.*, 1992, **31**, 1941.
3 (*a*) V. W.-W. Yam, C.-H. Lam, W. K.-M. Fung and K.-K. Cheung, *Inorg. Chem.*, 2001, **40**, 3435; (*b*) V. W.-W. Yam, C.-H. Lam and K.-K. Cheung, *Chem. Commun.*, 2001, 545; (*c*) V. W.-W. Yam, C.-L. Chan and K.-K. Cheung, *J. Chem. Soc., Dalton Trans.*, 1996, 4019; (*d*) V. W.-W. Yam, C.-K. Li and C.-L. Chan, *Angew. Chem., Int. Ed.*, 1998, **37**, 2857; (*e*) V. W.-W. Yam, C.-L. Chan, C.-K. Li and K. M.-C. Wong, *Coord. Chem. Rev.*, 2001, **216–217**, 173; (*f*) V. W.-W. Yam, Y.-L. Pui, K. M.-C. Wong and K.-K. Cheung, *Chem. Commun.*, 2000, 1751; (*g*) V. W.-W. Yam, Y.-L. Pui and K.-K. Cheung, *Inorg. Chem.*, 2000, **39**, 5741; (*h*) V. W.-W. Yam, Y.-L. Pui and K.-K. Cheung, *New J. Chem.*, 1999, **23**, 1163; (*i*) V. W.-W. Yam, Y.-L. Pui and K.-K. Cheung, *J. Chem. Soc., Dalton Trans.*, 2000, 3658.
4 (*a*) P. J. Bonasia, G. P. Mitchell, F. J. Hollander and J. Arnold, *Inorg. Chem.*, 1994, **33**, 1797; (*b*) K. Tang, X. Jin, H. Yan, X. Jie, C. Liu and Q. Gong, *J. Chem. Soc., Dalton Trans.*, 2001, 1374.
5 M. Lusser and P. Peringer, *Polyhedron*, 1985, **4**, 1997.
6 D. D. Perrin and W. L. F. Armarego, *Purification of Laboratory Chemicals*, Pergamon, Oxford, 3rd edn., 1988.
7 R. R. Gagńe, C. A. Koval and G. C. Lisensky, *Inorg. Chem.*, 1980, **19**, 2854.
8 D. Gewirth, Z. Otwinowski and W. Minor, *The HKL Manual-A Description of Programs DENZO, XDISPLAYF, and SCALEPACK*, Yale University, New Haven, USA, 1995.
9 G. M. Sheldrick, SHELX-97, Programs for Crystal Structure Analysis (release 97-2), University of Göttingen, Germany, 1997.
10 (*a*) P. T. Wood, W. T. Pennington and J. W. Kolis, *J. Chem. Soc., Chem. Commun.*, 1993, 235; (*b*) J. F. Corrigan and D. Fenske, *Chem. Commun.*, 1996, 943; (*c*) D. Fenske, N. Zhu and T. Langetepe, *Angew. Chem., Int. Ed.*, 1998, **37**, 2640; (*d*) S. P. Huang and M. G. Kanatzidis, *Inorg. Chem.*, 1991, **30**, 1455; (*e*) A. A. M. Aly, D. Neugebauer, O. Orama, U. Schubert and H. Schmidbaur, *Angew. Chem., Int. Ed. Engl.*, 1978, **17**, 125; (*f*) Z. Huang, X. Lei, M. Hong and H. Liu, *Inorg. Chem.*, 1992, **31**, 2990; (*g*) X. Jin, K. Tang, W. Liu, H. Zeng, H. Zhao, Y. Ouyang and Y. Tang, *Polyhedron*, 1996, **15**, 1207; (*h*) P. Perez-Lourido, J. A. Garcia-Vazquez, J. Romero, A. Sousa, E. Block, K. P. Marcesca and J. Zubieta, *Inorg. Chem.*, 1999, **38**, 538; (*i*) G. Henkel, P. Betz and B. Krebs, *Angew Chem., Int. Ed. Engl.*, 1987, **26**, 145; (*j*) M. A. Ansari, J. C. Bollinger and J. A. Ibers, *Inorg. Chem.*, 1993, **32**, 1746.